Chapter 17
Opacity

In this chapter we deal with the material function $\kappa(\varrho, T)$. While for the equation of state it was possible to use certain approximations (for instance, that of a perfect gas) without introducing too much error, this is almost impossible for the opacity. Although there are similar approximations (such as those for electron scattering or free–free transitions) they never hold for the whole star and are used only in simplifying approaches. Therefore, nowadays, when solving the stellar-structure equations, one uses numerical opacity tables for different chemical mixtures, which give $\kappa(\varrho, T)$ in the full range of ϱ and T.

In the following we describe the basic processes that contribute to the opacity and give approximate analytic formulae without deriving them from quantum mechanics. The reader who wants to learn more of the methods by which opacities are computed is referred to Weiss et al. (2004) and to the original papers quoted there.

17.1 Electron Scattering

If an electromagnetic wave passes an electron, the electric field makes the electron oscillate. The oscillating electron represents a classical dipole that radiates in other directions, i.e. the electron scatters part of the energy of the incoming waves. The weakening of the original radiation due to scattering is equivalent to that by absorption, and we can describe it by way of a cross section at frequency ν per unit mass (which we called κ_ν in Sect. 5.1). This can be calculated classically giving the result

$$\kappa_\nu = \frac{8\pi}{3}\frac{r_\mathrm{e}^2}{\mu_\mathrm{e} m_\mathrm{u}} = 0.20\,(1+X), \tag{17.1}$$

where r_e is the classical electron radius, X the mass fraction of hydrogen, and the constant is in $\mathrm{cm}^2\,\mathrm{g}^{-1}$. The term $\mu_\mathrm{e} m_\mathrm{u}$ arises because κ_ν is taken per unit mass; and μ_e is replaced by (4.30). Since κ_ν does not depend on the frequency, we immediately obtain the Rosseland mean for electron scattering:

R. Kippenhahn et al., *Stellar Structure and Evolution*, Astronomy and Astrophysics Library, DOI 10.1007/978-3-642-30304-3_17, © Springer-Verlag Berlin Heidelberg 2012

$$\kappa_{\rm sc} = 0.20\,(1+X)\,{\rm cm}^2\,{\rm g}^{-1}\,. \tag{17.2}$$

The "Thomson scattering" just described neglects the exchange of momentum between electron and radiation. If this becomes important, then κ_ν will be reduced compared to the value given in (17.1), though this effect plays a role only at temperatures sufficiently high for the scattered photons to be very energetic. In fact during the scattering process the electron must obtain such a large momentum that its velocity is comparable to c, say $v \gtrsim 0.1c$ for (17.2) to become a bad approximation. The momentum of the photon is $h\nu/c$, which after scattering is partly transferred to the electron, $m_{\rm e}v \sim h\nu/c$. Therefore relativistic corrections ("Compton scattering") become important if the average energy of the photons is $h\nu \gtrsim 0.1 m_{\rm e}c^2$. For $h\nu$ we take the frequency at which the Planck function has a maximum; then according to Wien's law this is at $h\nu = 4.965\,kT$, and the full Compton scattering cross section has to be taken into account if $T > 0.1 m_{\rm e}c^2/(4.965k)$, or roughly $T > 10^8$ K. In fact even at $T = 10^8$ K Compton scattering reduces the opacity by only 20 % of that given by (17.2).

17.2 Absorption Due to Free–Free Transitions

If during its thermal motion a free electron passes an ion, the two charged particles form a system which can absorb and emit radiation. This mechanism is only effective as long as electron and ion are sufficiently close. Now, the mean thermal velocity of the electrons is $v \sim T^{1/2}$, and the time during which they form a system able to absorb or emit is proportional to $1/v \sim T^{-1/2}$; therefore, if in a mass element the numbers of electrons and ions are fixed, the number of systems temporarily able to absorb is proportional to $T^{-1/2}$.

The absorption properties of such a system have been derived classically by Kramers, who calculated that the absorption coefficient per system is proportional to $Z^2\nu^{-3}$, where Z is the charge number of the ion. We therefore expect the absorption coefficient κ_ν of a given mixture of (fully ionized) matter to be

$$\kappa_\nu \sim Z^2 \varrho T^{-1/2} \nu^{-3}\,. \tag{17.3}$$

Here the factor ϱ appears because for a given mass element the probability that two particles are accidentally close together is proportional to the density.

For the determination of the Rosseland mean κ of this absorption coefficient we make use of a simple theorem which can be easily proved by carrying out the integration (5.19): a factor ν^α contained in κ_ν gives a factor T^α in κ. With this and with (17.3) we find

$$\kappa_{\rm ff} \sim \varrho T^{-7/2}\,. \tag{17.4}$$

All opacities of the form (17.4) are called *Kramers opacities* and give only a classical approximation. One normally multiplies the Kramers formula (17.4) by

a correction factor g, the so-called *Gaunt factor*, in order to take care of the quantum-mechanical correction (see, for instance, Weiss et al. 2004). In (17.4) we have still omitted the factor Z^2 which appears in (17.3). In general, one has a mixture of different ions, and therefore one has to add the contributions of the different chemical species. The (weighted) sum over the values of Z^2 is taken into the constant of proportionality in (17.4), which then depends on the chemical composition. For a fully ionized mixture a good approximation is given by

$$\kappa_{\rm ff} = 3.8 \times 10^{22}(1+X)[(X+Y)+B]\varrho T^{-7/2} \,, \tag{17.5}$$

with the numerical constant in cgs. The mass fractions of H and He are X and Y, respectively. Here the factor $1+X$ arises, since $\kappa_{\rm ff}$ must be proportional to the electron density–which is proportional to $(1+X)\varrho$. The term $(X+Y)$ in the brackets can be understood in the following way: there are $X/m_{\rm u}$ hydrogen ions and $Y/(4m_{\rm u})$ helium ions. The former have the charge number 1, the latter the charge number 2. But since $\kappa_\nu \sim Z^2$ [see (17.3)], when adding the contributions of H and He to the total absorption coefficient, we obtain the factor $X/m_{\rm u} + 4Y/(4m_{\rm u}) = (X+Y)m_{\rm u}$. Correspondingly the term B gives the contribution of the heavier elements:

$$B = \sum_i \frac{X_i Z_i^2}{A_i} \,, \tag{17.6}$$

where the summation extends over all elements higher than helium and A_i is the atomic mass number.

17.3 Bound–Free Transitions

We first consider a (neutral) hydrogen atom in its ground state, with an ionization energy of χ_0, i.e. a photon of energy $h\nu > \chi_0$ can ionize the atom. Energy conservation then demands that

$$h\nu = \chi_0 + \frac{1}{2}m_{\rm e}v^2 \,, \tag{17.7}$$

where v is the velocity of the electron released (relative to the ion, which is assumed to be at rest before and after ionization).

If we define an absorption coefficient a_ν per ion ($a_\nu = \kappa_\nu \varrho / n_{\rm ion}$), we expect $a_\nu = 0$ for $\nu < \chi_0/h$ and $a_\nu > 0$ for $\nu \geq \chi_0/h$. Classical considerations similar to those which lead to the Kramers dependence (17.3) of κ_ν for free–free transitions give $a_\nu \sim \nu^{-3}$ for $\nu \geq \chi_0/h$. Quantum-mechanical corrections can again be taken into account by a Gaunt factor (see, for instance, Weiss et al. 2004). The absorption coefficient of the hydrogen atom in its ground state has a frequency dependence as given in Fig. 17.1a. But if we have neutral hydrogen atoms in different stages of excitation, the situation is different: an atom in the first excited stage has an

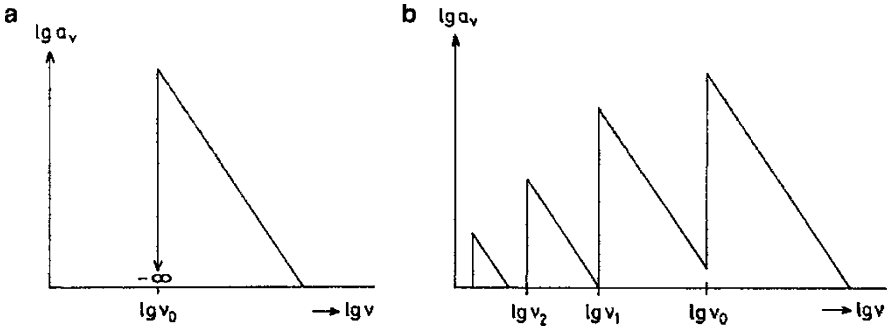

Fig. 17.1 (**a**) The absorption coefficient a_ν of a hydrogen atom in the ground state as a function of the frequency ν; $\nu_0 = \chi_0/h$ (**b**) The absorption coefficient of a mixture of hydrogen atoms in different stages of excitation

absorption coefficient $a_\nu = 0$ for $h\nu < \chi_1$, where χ_1 is the energy necessary to ionize a hydrogen atom from the first excited state, while $a_\nu \sim \nu^{-3}$ for $h\nu \geq \chi_1$. The absorption coefficient κ_ν for a mixture of hydrogen atoms in different states of excitation is a superposition of the a_ν for different stages of excitation. The resulting κ_ν is a sawtooth function, as indicated in Fig. 17.1b. In order to obtain κ_ν for a certain value of the temperature T, one has to determine the relative numbers of atoms in the different stages of excitation by the Boltzmann formula; then their absorption coefficients a_ν, weighted with their relative abundances, are to be summed. To obtain the Rosseland mean one has to carry out the integration (5.19).

If there are ions of different chemical species with different degrees of ionization, one has to sum the functions a_ν for all species in all stages of excitation and all degrees of ionization before carrying out the Rosseland integration. An important source of opacity are bound–free transitions of neutral hydrogen atoms, in which case the opacity must be proportional to the number of neutral hydrogen atoms and κ can be written in the form

$$\kappa_{\rm bf} = X(1-x)\tilde{\kappa}(T)\ . \tag{17.8}$$

Here $\tilde{\kappa}(T)$ is obtained by Rosseland integration over (weighted) sums of functions a_ν for the different stages of excitation, while x is the degree of ionization as defined in Sect. 14.2. The function $\tilde{\kappa}(T)$ is plotted in Fig. 17.2.

17.4 Bound–Bound Transitions

For absorption by an electron bound to an ion, more than just the bound–free transitions discussed in Sect. 17.3 contribute to the opacity. If, after absorption of a photon from a directed beam, the electron does not leave the atom but jumps to a

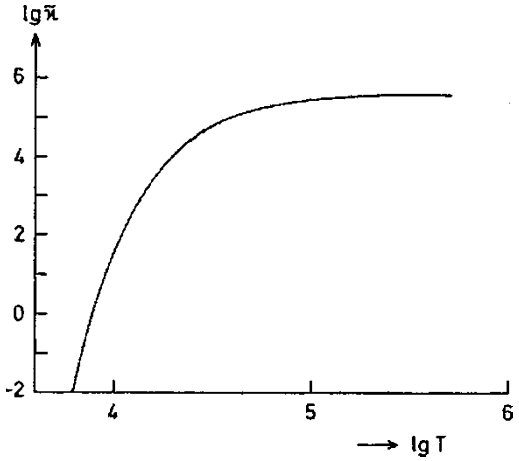

Fig. 17.2 The function $\tilde{\kappa}(T)$ of (17.8), where $\tilde{\kappa}$ is in $\mathrm{cm}^2\,\mathrm{g}^{-1}$ and T in K

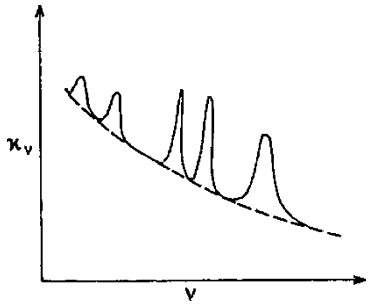

Fig. 17.3 Bound–bound transitions contributing to the opacity κ_ν

higher bound state, the energy will later on be re-emitted in an arbitrary direction, so that the intensity of the directed beam is weakened. This mechanism is effective only at certain frequencies, and one would expect that absorption in a few lines gives only a small contribution to the overall opacity; however, the absorption lines in stars are strongly broadened by collisions, and as one can see in Fig. 17.3, they can occupy considerable regions of the spectrum. Bound–bound absorption can become a major contribution to the (Rosseland mean) opacity if $T < 10^6\,\mathrm{K}$. It can then increase the total opacity by a factor 2, while for higher temperatures (say $T \approx 10^7\,\mathrm{K}$) the contribution of bound–bound transitions to the total opacity is much smaller (10 %). Calculation of the absorption coefficients due to bound-bound transitions obviously requires detailed knowledge about the energy levels of all atoms and ions, all mechanisms that lead to line broadening, and of all the transition probabilities. In addition, occupation levels and ionization levels have to be known, which links the calculation of opacities closely to that of the equation of state. Such calculations have again to be done in separate calculations by specialists in atomic physics.

17.5 The Negative Hydrogen Ion

Hydrogen can become a source of opacity in another way, by forming negative ions: a neutral hydrogen atom is polarized by a nearby charge and can then attract and bind another electron. This is possible since there exists a bound state for a second electron in the field of a proton, though this second electron is only loosely bound–the absorption of photons with $h\nu > 0.75\,\mathrm{eV}$ is sufficient for its release. This energy is very small compared to the 13.6 eV ionization energy for neutral hydrogen and allows photons with $\lambda < 1655\,\mathrm{nm}$ (infrared) to be absorbed, giving rise to a bound–free transition. The photon energy goes into the ionization energy and kinetic energy of the free electron in the same way as indicated in (17.7). The number of negative hydrogen ions in thermodynamic equilibrium is given by the Saha formula (14.17), where the ionization potential χ_r is the binding energy of the second electron. Replacing the partition functions by the statistical weights, we have $u_{-1} = 1$ for the negative ion and $u_0 = 2$ for neutral hydrogen; hence the Saha equation gives

$$\frac{n_0}{n_{-1}} P_\mathrm{e} = 4 \frac{(2\pi m_\mathrm{e})^{3/2} (kT)^{5/2}}{h^3} \mathrm{e}^{-\chi/kT} \,, \tag{17.9}$$

with $\chi = 0.75\,\mathrm{eV}$. If we use $n_0 = (1-x)\varrho X/m_\mathrm{u}$, where x is the degree of ionization of hydrogen as defined in (14.18) and X the weight fraction of hydrogen, we find

$$n_{-1} = \frac{1}{4} \frac{h^3}{(2\pi m_\mathrm{e})^{3/2} (kT)^{5/2} m_\mathrm{u}} P_\mathrm{e} (1-x) X \varrho \mathrm{e}^{\chi/kT} \,. \tag{17.10}$$

Now, for an absorption coefficient a_ν per H^- ion, it follows that $\kappa_\nu = a_\nu n_{-1}/\varrho$, which implies that the Rosseland mean is described by

$$\kappa_{\mathrm{H}^-} = \frac{1}{4} \frac{h^3}{(2\pi m_\mathrm{e})^{3/2} (kT)^{5/2} m_\mathrm{u}} P_\mathrm{e} (1-x) X \, a(T) \mathrm{e}^{\chi/kT} \,, \tag{17.11}$$

where $a = a(T)$ is obtained from a_ν by Rosseland integration (5.19). The opacity $\kappa_\mathrm{H}-$ is proportional to n_{-1}, which in turn is proportional to $n_0 n_\mathrm{e}$ (or $n_0 P_\mathrm{e}$), since the H^- ions are formed from *neutral* hydrogen atoms and free electrons.

For a completely neutral, pure hydrogen gas there would be no free electrons and therefore no H^- ions. If now the temperature is increased and the hydrogen becomes slightly ionized, giving $n_\mathrm{e} \sim X$, the free electrons can combine with neutral hydrogen atoms. One therefore would expect an increase of κ as long as $1 - x$ is not too small.

The situation is different in the case of a more realistic mixture of stellar material. Heavier elements have lower ionization potentials (a few eV) and provide electrons even at relatively low temperatures; hence, although there is only a small mass fraction of heavier elements, they determine the electron density at low temperatures where hydrogen is neutral. When the elements heavier than helium are singly ionized (say from 3,000 K to 5,000 K) one has

$$n_{\mathrm{e}} = \varrho\,[xX + (1 - X - Y)/A]/m_{\mathrm{u}}\,, \tag{17.12}$$

where $\varrho(1 - X - Y)/(Am_{\mathrm{u}})$ is the number density of atoms of higher elements ("metals") of mean mass number A. Even if the metals constitute only a small percentage in weight (and number), they still determine the opacity as long as $1 - X - Y > xXA$ (which becomes very small for low temperatures where x is small). The metal content can therefore be of great influence on κ for the surface layers and thus the outer boundary conditions of stars.

17.6 Conduction

Electrons, like all particles, can transport heat by conduction. Their contribution to the total energy transport can normally be neglected compared to that of photons, since the conductivity is proportional to the mean free path ℓ, and in normal (non-degenerate) stellar material $\ell_{\mathrm{photon}} \gg \ell_{\mathrm{particle}}$.

However, conduction by electrons becomes important in the dense degenerate regions in the very interior of evolved stars, as well as in white dwarfs. The reason is that in the case of degeneracy, all quantum cells in phase space below p_{F} are filled up, and electrons, when approaching ions and other electrons, have difficulty exchanging their momentum. This is equivalent to saying that "encounters" are rare or that the mean free path is large. In Sect. 5.2 we saw that the contribution to conduction can be formally taken into account in the equation of radiative transport by defining a "conductive opacity" κ_{cd}, as in (5.24). If κ_{rad} is the Rosseland mean of the (radiative) opacity, then conduction reduces the "total" opacity κ, as can be seen from (5.25):

$$\frac{1}{\kappa} = \frac{1}{\kappa_{\mathrm{rad}}} + \frac{1}{\kappa_{\mathrm{cd}}}\,. \tag{17.13}$$

The thermal conductivity of the electron component of a gas is mainly determined by collisions between electrons and ions, but electron–electron collisions can also be important. Analytic formulae can be found in Weiss et al. (2004), while tables of the thermal conductivity due to electrons in stellar material have been computed first by Hubbard and Lampe (1969). They list the conductivities of a pure hydrogen gas, a mixture of pure helium and pure carbon, a solar composition, and a mixture typical for the core of an evolved star. More recent work is published by Itoh and co-workers (Itoh et al. 1983) and Potekhin et al. (1999) for variable chemical mixtures.

The later source, which provides conductive opacities for any ion charge, was used to plot Fig. 17.4, which shows the dependence of the conductive opacity on density for a given temperature. For extremely strong degeneracy, κ_{cd} is proportional to $\varrho^{-2}T^2$.

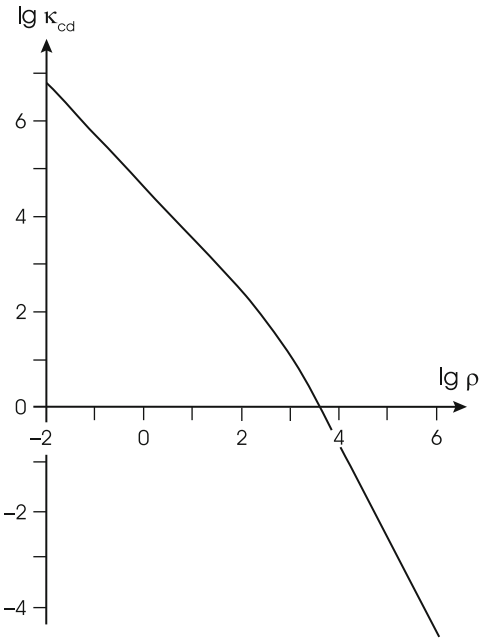

Fig. 17.4 The "conductive opacity" κ_{cd} (in $cm^2\,g^{-1}$) of a hydrogen gas at $T = 10^7$ K against the density ϱ (in $g\,cm^{-3}$) (Data from Potekhin et al. 1999)

17.7 Molecular Opacities

For temperatures below $\approx 10,000$ K the formation of molecules in the envelopes of cool stars becomes increasingly important. Due to their rich system of energy levels, corresponding to the various states of rotational and vibrational excitation, they are important absorbers. They contribute significantly to the opacity below $\approx 5,000$ K and begin to dominate it for $T \lesssim 3,000$ K. The importance of any absorber for the Rosseland mean opacity depends primarily on its absorption properties and not so much on its abundance. This is even more true for molecules and is the reason why Ti, which is three orders of magnitudes less abundant than oxygen, dominates–along with the water molecule–the opacity in the form of TiO as long as there is enough oxygen available for its formation. This is normally the case, unless there is more carbon than oxygen, in which case the oxygen is bound in CO molecules. In that case, other carbon molecules, such as C_2, CN, or C_2H_2, dominate.

Obviously, molecular opacities depend on atomic abundances, on the formation and stability of the various molecules, and finally on their energy level spectrum. This problem is sufficiently complicated that it can again be treated only in separate calculations including atomic and molecular physics, thermodynamics, and chemical processes. The results are again made available in tabular form for the stellar modelling. The largest sets of such tables has been provided by Alexander and Ferguson (Alexander and Ferguson 1994; Ferguson et al. 2005). The calculations consider more than 30 elements, over 50 molecules, and some 800 million atomic and molecular lines. In addition, absorption by dust grains is also

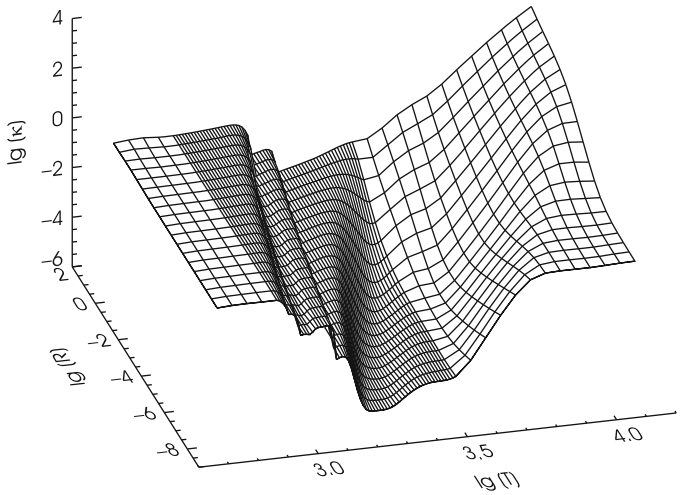

Fig. 17.5 The Rosseland mean of the opacity κ (in $\mathrm{cm}^2\,\mathrm{g}^{-1}$) as a function of $R = \varrho/T_6^3$ (in $\mathrm{g\,cm}^{-3}$, since $T_6 = T/10^6\,\mathrm{K}$) and T (in K) for a mixture of $X = 0.70$, $Y = 0.29$, $Z = 0.01$, using data for atomic, molecular, and dust opacity from Ferguson et al. (2005)

included. They dominate below 1500 K, temperatures which are usually found in stellar atmospheres only.

Figure 17.5 shows the total Rosseland opacity for a mixture with 70 % hydrogen and 1 % of metals. The varying density of the grid lines reflects the density of the (R, T) points computed for the table [In this and the following, similar figures, the quantity $R = \varrho/T_6^3$ (with $T_6 = T/10^6\,\mathrm{K}$) has been used as this has become customary in the opacity community. This quantity is roughly constant in large parts of main-sequence stars. This R must not be confused with the stellar radius and is used with this meaning in this chapter only.]. In regions of many different opacity sources the opacities were calculated at many temperatures and densities. At higher temperatures, atomic absorption dominates; the steep rise to the right is mainly caused by the H^- ion. The "shoulder" around $\lg T = 3.4$ and low R is caused by the first formation of molecules, such as CO, NO, and H_2. The first sharp rise at lower temperatures after we passed the minimum around $\lg T = 3.3$ is due to formation of TiO and H_2O, which is followed by a slight decrease in κ once temperatures are too low to allow many excited states in the molecules. The various maxima at even lower temperatures are caused by different grains appearing and disappearing. For example, the one around $\lg T = 3.1$ is due to Al_2O_3 and $CaTiO_3$. Solid silicates and iron grains form at even lower temperatures. Each of these features is also present at higher densities, but then already occurring at higher temperatures.

Such low temperatures, where molecular or even dust absorption dominates, are usually found in stars only in convective envelopes. However, the outermost parts of these envelopes are highly superadiabatic (Chap. 7), such that $\nabla \lesssim \nabla_{\mathrm{rad}}$, and therefore the opacities determine the temperature stratification even in this case.

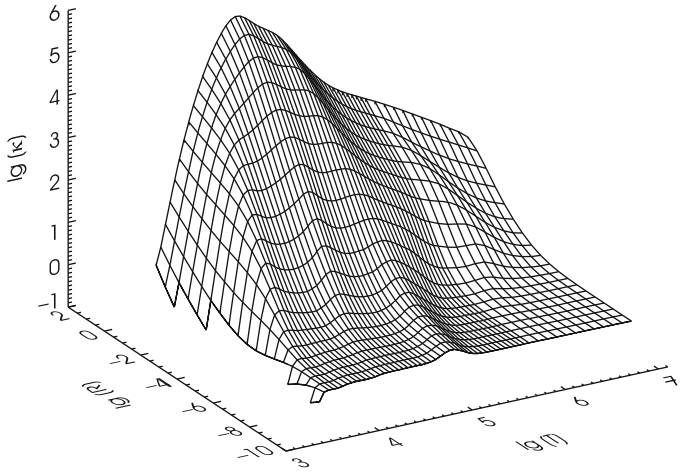

Fig. 17.6 The Rosseland mean of the opacity κ (in $\mathrm{cm}^2\,\mathrm{g}^{-1}$) as a function of $R = \varrho/T_6^3$ (in $\mathrm{g\,cm}^{-3}$, since $T_6 = T/10^6\,\mathrm{K}$) and T (in K) for a mixture with a hydrogen and helium content $X = 0.70$, $Y = 0.29$. These are opacities calculated by the OPAL project at Lawrence Livermore National Laboratory (Rogers and Iglesias 1992; Iglesias and Rogers 1996). The dominant absorption mechanisms at different parts of the model are discussed in the text. The continuation towards higher temperatures is shown in Fig. 17.7

17.8 Opacity Tables

In view of the complexity of modern opacity calculations, the basic considerations of Sects. 17.1–17.6 are not sufficient for calculating accurate stellar models. Instead, specialized groups have published extensive tables of opacities for different chemical mixtures over a wide range of temperatures and densities. Each group, however, may specialize on one specific aspect. The *Opacity Project* (Mendoza et al. 2007) and the Livermore *OPAL* group concentrate on atomic absorption important for higher temperatures (Fig. 17.6); the Wichita group (Alexander and Ferguson) on molecular and dust absorption for temperatures below $10^4\,\mathrm{K}$, and finally Itoh, Pothekin, and others on electron conduction. These various sources then have to be combined to opacity tables covering the whole stellar structure. Indeed, the low-and high-temperature opacities, which are shown in Figs. 17.5 and 17.6, agree very well in the overlapping temperature range. The conductive opacities can finally be added by use of (17.13).

In Fig. 17.7 we give a graphical representation of such a combined opacity table for a mixture with a metal fraction of 0.01 and a hydrogen content of 0.70. Figures 17.6 and 17.5 show the corresponding individual parts for the same mixture.

Indeed one sees that, over the whole range of arguments, $\kappa(R, T)$ is a rather complicated function. In order to give a feeling for the parts of the plotted surface that are relevant to stars, we discuss a model of the present Sun, which is plotted in Fig. 17.7 (thick solid line). We are using only the $T - \varrho$ structure; the chemical

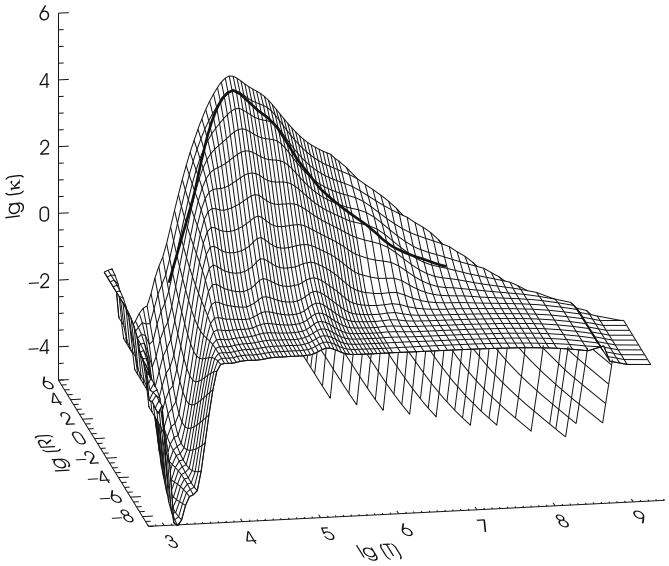

Fig. 17.7 Combination of the opacity κ shown in Figs. 17.6 and 17.5, and of electron conduction opacities as in Fig. 17.4. The latter is a steeply declining function of ϱ (or R) and can be seen "from below" in the back of the figure. Electron scattering provides the flat region in the right foreground. The *thick solid line* represents the $T - \varrho$ structure of a solar model (for details see text)

composition of the Sun is in fact quite different from that of the table. For example, in the solar centre, $X \approx 0.34$, and at the surface, the composition is $X = 0.737$, $Y = 0.245$, and $Z = 0.018$. Nevertheless, the main features are still visible. Note also, that R indeed is rather constant throughout the solar interior, although ϱ varies by eight orders of magnitude.

The model starts with the photospheric values $\lg T = 3.76$, $\lg \varrho = -6.58$ (in cgs), or $\lg R = 0.14$. The corresponding point lies on the left end of the thick solid line in Fig. 17.7 and on the rising slope on the right of Fig. 17.5, where molecular opacities are still contributing. On moving deeper into the Sun the opacity sharply increases owing to the onset of hydrogen ionization, which provides the electrons for H^- formation as described in Sect. 17.5, and the opacity rises by several powers of 10 until it reaches a maximum value. This occurs when an appreciable amount of hydrogen becomes ionized and is not available for H^- formation, because the factor $1 - x$ in (17.11) reduces the opacity. In the regions below, bound–free transitions become the leading opacity source and still further inwards free–free transitions take over. There a simple power law seems to be a good approximation, as indicated in (17.4). Note that in the logarithmic representation the opacity surface for a power law is just a plane. Equation (17.4) therefore corresponds to a tangential plane which osculates the opacity surface. The line for the interior remains in the domain of free–free transitions. The region of dominant electron scattering is the horizontal plateau

in the foreground on the right of Fig. 17.7 at the foot of the "kappa mountain". In this figure the region where electron conduction reduces the (total) opacity is hidden behind the mountain ridge and can be seen only "from below" as the plane dropping below the electron scatter region at high densities. At the highest temperatures, κ is reduced below the electron-scattering value due to Compton scattering as mentioned in Sect. 17.1.

In order to find the value of $\kappa(\varrho, T, X_i)$ for a given point with ϱ_0, T_0, X_{i0} in a star, one has to interpolate in different opacity tables (for different compositions X_i) for the arguments ϱ_0, T_0 and then between these tables for X_{i0}. Tables are calculated not only for different $(X,\ Y,\ Z)$ combinations, but also for different relative metal ratios within the Z-group. When combining opacities from different sources, as is almost always necessary, tables for identical metal mixtures are preferable, and great care in the interpolation has to be taken.

Note finally, that the temperature and density range even of the combined opacity table is limited. In particular the high density limit is critical as low-mass stars have structures that reach high densities at rather low temperatures. The reason for the lack of available opacity data lies in the equation of state: this is the region where complicated non-ideal gas effects (Sect. 16.6) prevent an accurate calculation of the thermodynamic state of the gas, and therefore the calculation of opacities becomes impossible. In practical stellar evolution calculations, such a situation asks for the creativity of the modeller to somehow supplement the missing data.